Competition between Stepwise Polarization Switching and Chirality Coupling in Ferroelectric GeS Nanotubes

Hao-Chen Wang(王浩臣)[1,2], Zhi-Hao Wang(王智灏)[2], Xuan-Yan Chen(陈宣言)[2], Su-Huai Wei(魏苏淮)[2*], Wenguang Zhu(朱文光)[1*], and Xie Zhang(张燮)[2*]

[1]*School of Physical Sciences, University of Science and Technology of China, Hefei 230026, China*
[2]*Beijing Computational Science Research Center, Beijing 100193, China*

(Received 23 February 2023; accepted manuscript online 13 March 2023)

Ferroelectricity of group-Ⅳ chalcogenides MX ($M=$ Ge, Sn; $X=$ Se, S) monolayers has been extensively investigated. However, how the ferroelectricity evolves in their one-dimensional nanotubes remains largely unclear. Employing an accurate deep-learning interatomic potential of first-principles precision, we uncover a general stepwise mechanism for polarization switching in zigzag and chiral GeS nanotubes, which has an energy barrier that is substantially lower than the one associated with the conventional one-step switching mechanism. The switching barrier (per atom) gradually decreases with increasing the number of intermediate steps and converges to a value that is almost independent of the tube diameter. In the chiral GeS nanotubes, the switching path of polarization with chirality coupling is preferred at less intermediate steps. This study unveils novel ferroelectric switching behaviors in one-dimensional nanotubes, which is critical to coupling ferroelectricity and chirality.

DOI: 10.1088/0256-307X/40/4/047701

Ferroelectric materials, due to the lack of inversion symmetry, possess spontaneous polarizations below a critical temperature, which can be reversed by external electric fields. The robust ferroelectricity was first discovered in bulk perovskites, e.g., $BaTiO_3$ [1] and $PbTiO_3$.[2] Ferroelectric materials are highly valuable in technological applications such as ultrasound and actuator devices.[3,4] However, when bulk ferroelectric materials were developed as electrically switchable memories, they could face difficulties in high-density integration and device miniaturization.[5] In recent years, two-dimensional (2D) ferroelectric materials have been discovered, including In_2Se_3,[6,7] $CuInP_2S_6$,[8] and group-Ⅳ chalcogenide monolayers,[9–11] which has opened the possibility of integrated nano-electronic devices and new computing architectures.

Compared to 2D ferroelectric materials, one-dimensional (1D) ferroelectric materials, such as nanowires, nanotubes, and nanoribbons, are expected to be superior for building high-density ferroelectric devices. In addition, the bending deformation in 1D structures may also affect the ferroelectric properties by impacting the Ginzburg coefficient of P^2, where P is the polarization. One-dimensional ferroelectricity has indeed been theoretically proposed in, e.g., van der Waals crystals $NbOX_3$ ($X=$ Cl, Br, I),[12] group-Ⅳ chalcogenide nanowires,[13] and perovskite nanotubes.[14,15] Experimentally, it has also been demonstrated that controlled fabrication of pure single-crystal 1D nanotubes is feasible.[16]

Ferroelectricity in low-dimensional materials is often investigated theoretically using density functional theory (DFT). DFT calculations can provide accurate results of electronic properties (e.g., spontaneous polarization and switching barriers of single domain), but may fall short on describing the macroscopic properties (e.g., nucleation and growth of domains and domain-wall dynamics[17–20]). Previous studies on the domain properties of prototypical perovskites[21–24] and 2D GeS monolayers[25] mostly focused on the domain-wall energy and the polarization in the vicinity of the interface. The impact of nanoscale ferroelectric domains on the polarization switching barriers has been rarely investigated, since it requires large systems and extended computation time that are usually beyond the capability of DFT. It is thus critical to develop a computationally efficient method to calculate ferroelectric switching barriers with the domain effects taken into account. Remarkable developments in machine-learning techniques in recent years have fueled the construction of highly accurate and transferrable interatomic potentials within the DFT level of accuracy.[26,27] The use of machine-learning potentials enables feasible simulations of large supercells, providing a powerful tool to investigate the ferroelectricity in nanoscale materials.[28,29]

In this work, we develop a highly accurate deep-learning interatomic potential for a prototypical 2D ferroelectric material GeS. The electronic contribution to the polarization is involved in the deep-learning potential through the training with DFT calculation data. We investigate the ferroelectric properties in different types of GeS nanotubes with the domain effects properly taken into account. For zigzag and chiral GeS nanotubes with different tube indices, we find that the formation energies of both nanotubes decrease with the tube diameters. We examine the kinetic switching paths of polarization in GeS nanotubes and discover a general stepwise switching mechanism with much lower energy barriers, which may apply

*Corresponding authors. Email: suhuaiwei@csrc.ac.cn; wgzhu@ustc.edu.cn; xiezhang@csrc.ac.cn
© 2023 Chinese Physical Society and IOP Publishing Ltd

to other ferroelectric materials as well. The switching barriers (per atom) decrease with the number of intermediate steps and converge to a value that is independent of the diameters. In chiral GeS nanotubes, there are two switching paths: (i) a chirality-coupling (CC) path and (ii) a non-chirality-coupling (NCC) path. At less intermediate steps, the switching barrier of the CC path is lower than that of the NCC one, making the coupling of ferroelectricity and chirality possible. This discovery constitutes an important basis for manipulating the coupling between ferroelectricity and chirality in chiral GeS nanotubes.

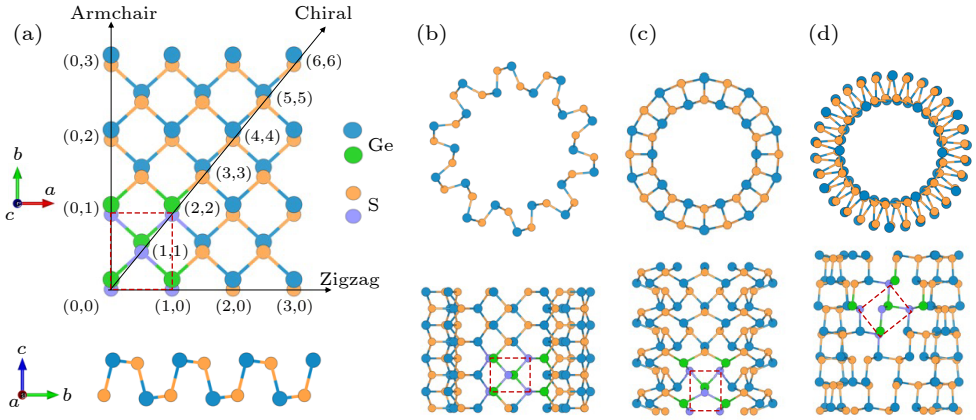

Fig. 1. Atomic structures of GeS monolayer and three types of nanotubes. (a) Top and side views of GeS monolayer. The unit cell is marked by a red dashed rectangle. Three ways of rolling along armchair, zigzag, and chiral directions are labeled as $(0, n)$, $(n, 0)$, and (n, n). (b)–(d) Top and side views of (b) armchair, (c) zigzag, and (d) chiral nanotubes.

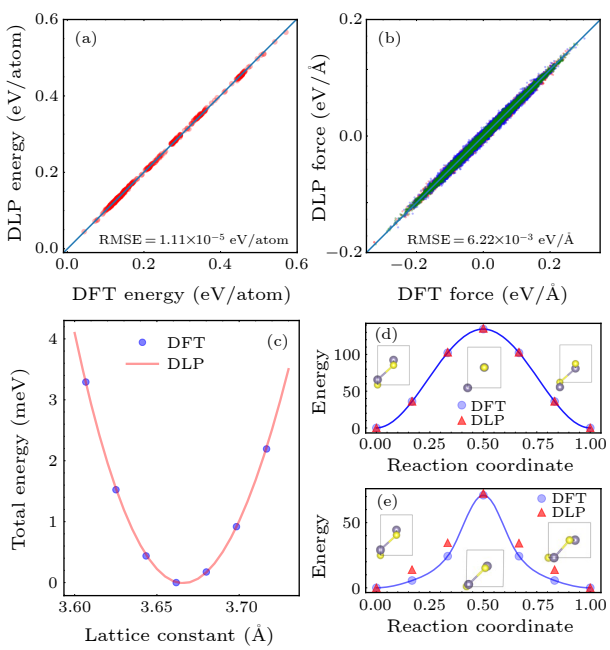

Fig. 2. Performance of the deep-learning potential (DLP). [(a), (b)] Comparisons of the (a) energy and (b) forces between DFT calculations and DLP predictions with respect to the same validation dataset. The energy values are referenced to that of the optimized 5×5 supercell. (c) Curves of energy vs lattice constant, calculated by DFT and the deep-learning potential. [(d), (e)] The 180° (d) and 90° (e) switching paths of polarization in GeS monolayer. The energies are in units of meV/atom. The insets show the atomic structures of the initial, transition, and final states.

GeS nanotubes can be constructed by rolling 2D GeS monolayers in different manners. In Fig. 1(a), we present the atomic structure of a GeS monolayer, in which the primitive cell (marked by the red dashed rectangle in the top view) consists of two Ge atoms and two S atoms. It was previously reported that spontaneous in-plane polarization exists along the armchair direction and it can be switched by 180° and 90° via electric fields.[30] We show three ways to roll the GeS monolayer, along the armchair, zigzag and chiral directions, which are labeled $(0, n)$, $(n, 0)$, and (n, n). The formed nanotubes are presented in Figs. 1(b)–1(d). In addition, we mark the unit cell of GeS monolayer with different colors to highlight it in the three types of nanotubes (see the red dashed rectangles). Based on the direction of in-plane polarization in the GeS monolayer, we find that there is no net polarization along the tube axis in armchair nanotubes, as it goes around the tube and cancels itself. Zigzag nanotubes are polarized along the tube axis, while chiral nanotubes have polarizations both along the tube axis and around the tube surface, forming a chiral structure of polarization [right-handed upward polarization in Fig. 1(d)]. This provides a platform to couple ferroelectricity and chirality.

We investigate the zigzag nanotube with a tube index $(250, 0)$ and chiral nanotube with $(240, 240)$, which consist of 1000 and 2400 atoms. The large size of these nanotubes allows us to consider the effect of polarization domains on kinetic switching of the polarization. We perform *ab initio* molecular dynamics (AIMD) simulations for a 5×5 supercell of GeS monolayer, and eleven datasets of different volumes are generated to cover a large sampling space. There are 95% of these data that are used to train the deep-learning potential and the rest 5% are used for validation.

In Figs. 2(a) and 2(b), we show a comparison of energies and forces between DFT calculations and deep-

learning predictions. The points of energies and forces are very close to the diagonal ones, and their root-mean-square errors (RMSE) presented in Figs. 2(a) and 2(b) are sufficiently small. As depicted in Fig. 2(c), the developed deep-learning potential accurately captures the energy dependence on the lattice constant in a wide range, which further proves the accuracy of the deep-learning potential.

For a key quantity of interest for ferroelectricity, we also calculate the ferroelectric switching barriers associated with two switching paths of polarization in GeS monolayer using nudged elastic band (NEB) simulations in Figs. 2(d) and 2(e). The insets present the atomic structures of initial, transition, and final states. In Fig. 2(d), Ge atoms collectively move downward along the path and the polarization is switched by 180°. In Fig. 2(e), Ge atoms collectively move toward lower right and the polarization is switched by 90°. The switching barriers from the deep-learning potential agree remarkably well with the ones from DFT calculations, which proves the accuracy of the deep-learning potential in capturing ferroelectric properties.

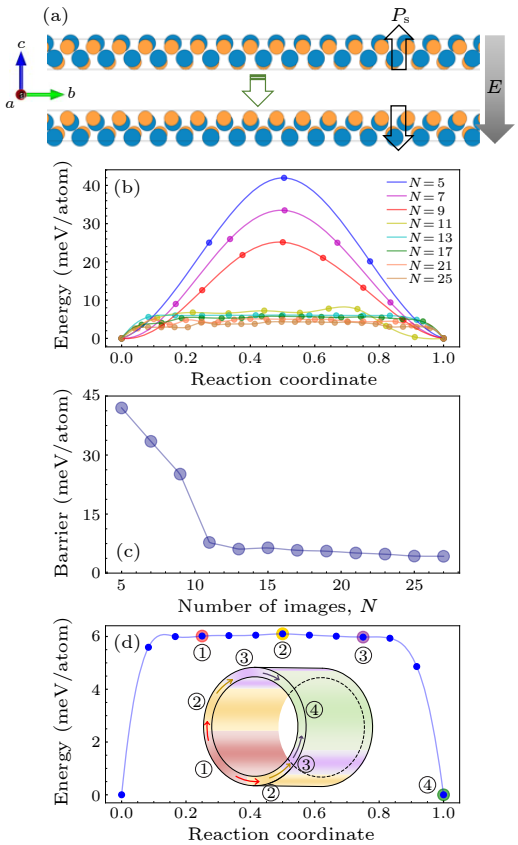

Fig. 3. Switching path and barrier in the zigzag $(250, 0)$ nanotube. (a) Initial and final states with the polarization along c and $-c$. (b) Minimum-energy paths of polarization switching with respect to the number of images N. (c) Energy barrier as a function of N. (d) Detailed stepwise switching path for the case of $N = 13$. The equally spaced four images are picked and the polarization is switched step by step around the tube surface $(1 \to 2 \to 3 \to 4)$.

We employ the developed potential to study the polarization switching in the zigzag nanotube with a tube index $(250, 0)$. The local atomic structures (front view) of the initial and final states are shown in Fig. 3(a). The polarization in this zigzag nanotube is along the c direction and is switched to $-c$ through this path. In the simplest switching path, all Ge atoms (in a single domain) move collectively downward in order to switch the polarization. Such a path, however, does not account for intermediate switching steps that may be triggered by the presence of multiple domains and domain walls, i.e., all Ge atoms in the tube do not necessarily move at once. In order to unveil more realistic and energetically more favorable switching paths of polarization, we investigate the dependence of the minimum-energy path (MEP) of polarization switching on the number of replica images in the NEB calculations.

In Fig. 3(b), the switching paths with different numbers of images, N, are presented. We find that the paths with less than 9 images exhibit only one peak and the barrier decreases with increasing N. As we further increase N, the MEPs of polarization switching become indistinctive, flat, and multi-peak. In Fig. 3(c), the switching barrier gradually decreases and converges to a small barrier that is substantially lower than the one at small N's (or the switching barrier in 2D GeS monolayer).

It can be further noticed that there is a qualitative change in the MEP of polarization switching when N changes from 9 to 11. At $N \leq 9$, the atoms move collectively at once to complete the switching process and the corresponding path has only one peak. However, when $N \geq 11$, the switching process involves multiple intermediate steps and the paths become more complex. In this case, only a fraction of the atoms move locally in each step (see the Supporting Information). This stepwise switching process takes the domain effects into account and drastically lowers the energy barrier. When the number of the intermediate steps becomes larger, growth of the interfaces between domains with different polarization states (domain walls) is observed. The appearance and expansion of the interface increase the energy of the system and reduce the barrier between two polarization states. In Fig. 3(d), we illustrate the stepwise switching mechanism and the expansion of domain walls around the tube surface with a case of $N = 13$ and label four representative intermediate switching steps 1–4 circled and different colors. The inset shows a schematic diagram of the zigzag nanotube and the stepwise switching pathway around the tube surface. We fill the inner space with different colors to address which parts are switched in each step. In the first picked image 1, only a quarter of the nanotube (red area) is switched compared to the initial state. From circled 1 to circled 2, the polarization switching propagates with the yellow areas being switched. Then two purple areas are switched from circled 2 to circled 3. Finally, the whole switching process is completed when the green part is switched in the fourth image (circled 4).

Next we investigate two switching paths of polarization in the chiral $(240, 240)$ nanotube. Because of the large size of the nanotube, only a fraction of the tube is displayed in Fig. 4(a). We mark the unit cell of GeS monolayer with black solid rectangles and the direction of rectangle (also the direction of polarization) is pointing toward upper right. This polarization can be decomposed as a su-

perposition of polarizations along the tube axis and around the tube surface [see Fig. 4(a)]. We call this chiral structure of polarization (right, up). Similarly, the final states of two different switching paths are shown in Figs. 4(b) and 4(c). Comparing the marked unit cells in Figs. 4(a)–4(c), we find the paths (a)→(b) and (a)→(c), i.e., structural transformations, correspond to the 180° and 90° switching of polarization in the 2D GeS unit cell [Figs. 2(d) and 2(e)]. In these two switching paths [(a)→(b) and (a)→(c)], the decomposed polarizations along the tube axis are both switched downward. However, for the polarization around the tube surface, the direction remains unchanged in the path (a)→(b), but is switched in the path a→c. Apparently, the chirality flips synchronously when the polarization along the tube axis is switched in the second path (a)→(c).

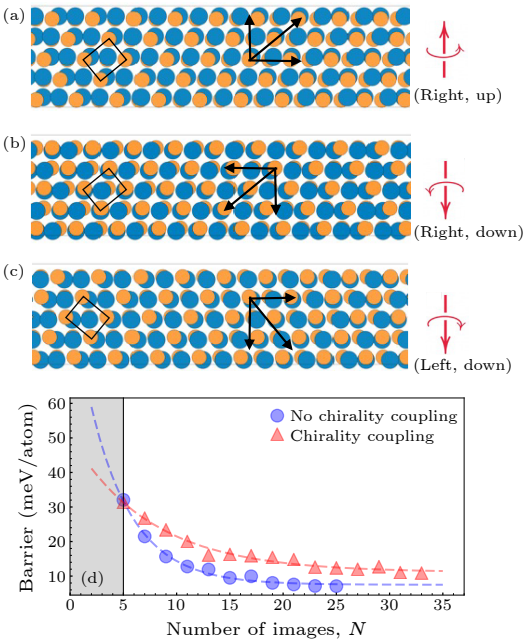

Fig. 4. Switching paths and barriers in the chiral (240, 240) nanotube. (a) Front views of the local atomic structure of the tube and the initial state of polarization. [(b), (c)] Final states of the two paths. The chirality changes in the path (a)→(b), while it does not in the path (a)→(c). The unit cell of the GeS monolayer is labeled by the black solid rectangle and the decompositions of the polarization are shown by the black arrows on the right side. (d) Switching barriers of the (a)→(b) and (a)→(c) paths with respect to the number of images N.

We perform NEB calculations with different numbers of replica images (N) and obtain the switching barriers as depicted in Fig. 4(d). The barriers of both switching paths decrease with increasing N and gradually converge. For the converged barrier, the NCC path [(a)→(b)] is energetically more favorable than the CC path [(a)→(c)]. However, when $N \leq 5$, the barrier of the CC path is lower, which means that the coupling of chirality is possible. Similar to Fig. 3(d), we analyze the atomic displacements in the switching process with $N = 21$. A similar stepwise switching mechanism is observed (see the Supporting Information). With $N \leq 5$, all atoms in the tube move collectively and the polarization is switched at once. This means that the path without chirality coupling is energetically more favorable in the stepwise switching process. Hence, in order to couple ferroelectricity and chirality, the stepwise switching path should be suppressed, which may be achieved by applying a very strong electric field.

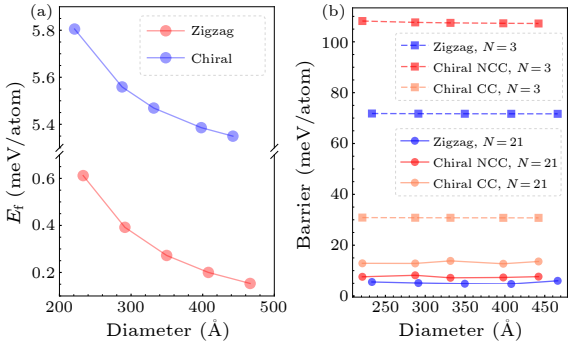

Fig. 5. (a) Formation energies of the zigzag and chiral nanotubes with different diameters. (b) Switching barriers in the zigzag and chiral nanotubes with $N = 3$ and $N = 21$.

Besides the zigzag (250, 0) and the chiral (240, 240) nanotubes, we also investigate nanotubes with different tube indices (see Methods in the Supporting Information). We define the formation energy by $E_f = E_{tube} - E_{ref}$, where E_{tube} (E_{ref}) is the energy of GeS nanotube (GeS monolayer with the same number of atoms). The formation energies of both zigzag and chiral nanotubes decrease as the tubes become larger; the zigzag nanotubes have lower formation energies than the chiral nanotubes of the same diameter [see Fig. 5(a)]. In Fig. 5(b), we calculate the barriers of switching paths in the zigzag nanotube [Fig. 3(a)] and the chiral nanotube (the NCC and CC paths in Fig. 4) of different diameters. $N = 3$ and $N = 21$ are adopted as representative cases for these calculations. Two important insights can be extracted from Fig. 5(b). First, the barriers (per atom) of all switching paths are independent of diameters. Despite the fact that the bending deformation enforced by the nanotube increases the Ginzburg coefficient of P^2 and then the switching barrier, this effect becomes negligible when the tube diameter becomes relatively larger. In this case, the switching barrier gradually approaches the value in the bending-free monolayer. Second, the competition between the CC and NCC paths is not affected by the diameter of the nanotube, but is primarily determined by the number of intermediate switching steps (the appearance of domain walls and their expansion).

In summary, we have studied the polarization switching paths and barriers with domain effects taken into account in zigzag and chiral GeS nanotubes using a newly developed highly accurate deep-learning potential. The switching barriers (per atom) are found to decrease with increasing the number of intermediate steps and converge to a value that is diameter-independent. Most notably, a general stepwise polarization switching mechanism with much lower energy barriers was identified, which is absent in single-domain switchings in ferroelectric materials. It may be feasible to experimentally observe the stepwise

switching mechanism in 2D ferroelectric materials using *in situ* microscopy (e.g., atomic force microscopy and piezoelectric force microscopy). In chiral nanotubes, chirality coupling is preferred in the one-step switching pathway, but is less favorable in the stepwise switching scenario with the appearance and expansion of domain walls. Our important insights elucidate a general stepwise polarization switching mechanism in ferroelectric systems (not only the nanotubes, but also monolayers or three-dimensional bulk materials) and lay the foundation of coupling ferroelectricity and chirality, which are expected to be generally applicable in low-dimensional ferroelectric materials.

Acknowledgements. This work was supported by the National Natural Science Foundation of China (Grant Nos. 52172136, 11991060, 12088101, and U2230402), and the Bohrium Cloud Platform (https://bohrium.dp.tech) of DP Technology. We acknowledge computational resources from the Beijing Computational Science Research Center.

References

[1] Smith M B, Page K, Siegrist T, Redmond P L, Walter E C, Seshadri R, Brus L E, and Steigerwald M L 2008 *J. Am. Chem. Soc.* **130** 6955
[2] Bhide V G, Deshmukh K G, Hegde M S 1962 *Physica* **28** 871
[3] Acosta M, Novak N, Rojas V, Patel S, Vaish R, Koruza J, Rossetti J G A, and Rödel J 2017 *Appl. Phys. Rev.* **4** 041305
[4] Gao J H, Xue D Z, Liu W F, Zhou C, and Ren X B 2017 *Actuators* **6** 24
[5] Mikolajick T, Schroeder U, and Slesazeck S 2020 *IEEE Trans. Electron. Devices* **67** 1434
[6] Ding W J, Zhu J B, Wang Z, Gao Y F, Xiao D, Gu Y, Zhang Z Y, and Zhu W G 2017 *Nat. Commun.* **8** 14956
[7] Zheng C, Yu L, Zhu L, Collins J L, Kim D, Lou Y, Xu C, Li M, Wei Z, Zhang Y, Edmonds M T, Li S, Seidel J, Zhu Y, Liu J Z, Tang W, and Fuhrer M S 2018 *Sci. Adv.* **4** eaar7720
[8] Liu F, You L, Seyler K L, Li X, Yu P, Lin J, Wang X, Zhou J, Wang H, He H, Pantelides S T, Zhou W, Sharma P, Xu X, Ajayan P M, Wang J, and Liu Z 2016 *Nat. Commun.* **7** 12357
[9] Chang K, Liu J, Lin H, Wang N, Zhao K, Zhang A, Jin F, Zhong Y, Hu X, Duan W, Zhang Q, Fu L, Xue Q, Chen X, and Ji S 2016 *Science* **353** 274
[10] Wang H and Qian X 2017 *2D Mater.* **4** 015042
[11] Higashitarumizu N, Kawamoto H, Lee C J, Lin B H, Chu F H, Yonemori I, Nishimura T, Wakabayashi K, Chang W H, and Nagashio K 2020 *Nat. Commun.* **11** 2428
[12] Zhang L, Tang C, Sanvito S, and Du A 2021 *npj Comput. Mater.* **7** 135
[13] Zhang J J, Guan J, Dong S, and Yakobson B I 2019 *J. Am. Chem. Soc.* **141** 15040
[14] Zhang X Y, Lai C W, Zhao X, Wang D Y, and Dai J Y 2005 *Appl. Phys. Lett.* **87** 143102
[15] Shimada T, Wang X, Kondo Y, and Kitamura T 2012 *Phys. Rev. Lett.* **108** 067601
[16] Xiang R, Inoue T, Zheng Y, Kumamoto A, Qian Y, Sato Y, Liu M, Tang D, Gokhale D, Guo J, and Hisama K 2020 *Science* **367** 537
[17] Shin Y H, Grinberg I, Chen I W, and Rappe A M 2007 *Nature* **449** 881
[18] Klomp A J, Khachaturyan R, Wallis T, Albe K, and Grunebohm A 2022 *Phys. Rev. Mater.* **6** 104411
[19] Ou Y J, Sun J, Li Y M, and Jiang A Q 2023 *Chin. Phys. Lett.* **40** 038501
[20] Zhao W, Fu Z, Deng J, Li S, Han Y, Li M R, Wang X, and Hong J 2021 *Chin. Phys. Lett.* **38** 037701
[21] Jin C F, Zhang S Q, Shen Z Q, and Li W L 2019 *Chin. Phys. Lett.* **36** 107701
[22] Zhang X, Wang B, Ji Y, Xue F, Wang Y, and Chen L Q 2023 *Acta Mater.* **242** 118351
[23] Lubk A, Gemming S, and Spaldin N A 2009 *Phys. Rev. B* **80** 104110
[24] Xu S Q, Zhang Y, Guo H Z, Geng W P, Bai Z L, and Jiang A Q 2017 *Chin. Phys. Lett.* **34** 027701
[25] Yan Y, Xiang M, Wang X, Xu T, and Xuan F 2022 *J. Appl. Phys.* **132** 074302
[26] Behler J 2016 *J. Chem. Phys.* **145** 170901
[27] Mueller T, Hernandez A, and Wang C 2020 *J. Chem. Phys.* **152** 050902
[28] Zhang J, Zhang F, Wei D, Liu L, Liu X, Fang D, Zhang G X, Chen X, and Wang D 2022 *Phys. Rev. B* **105** 094116
[29] Wu J, Bai L, Huang J, Ma L, Liu J, and Liu S 2021 *Phys. Rev. B* **104** 174107
[30] Wu M and Zeng X C 2016 *Nano Lett.* **16** 3236